



VERIFICATION OF WENO FOR HYPERBOLIC CONSERVATION LAWS

Nicholas D. P. da Silva

dicati@ufpr.br

Federal University of Paraná

Avenida Coronel Francisco Heráclito dos Santos, 100, 81530-900, Paraná, Curitiba, Brasil.

Rafael B. de R. Borges

rafael.borges@ime.uerj.br

Rio de Janeiro State University

Rua São Francisco Xavier, 524, 20550-900, Rio de Janeiro, Rio de Janeiro, Brasil.

Carlos H. Marchi

Luciano K. Araki

chmcf@gmail.com

lucaraki@ufpr.br

Federal University of Paraná

Avenida Coronel Francisco Heráclito dos Santos, 100, 81530-900, Paraná, Curitiba, Brasil.

Abstract. Verification is an important procedure to assess numerical schemes and its solutions. One of the most popular numerical scheme is the Weighted Essentially Nonoscillatory (WENO). This scheme is high-order accurate and presents high resolution. The purpose of this work is to assess numerical solutions of three hyperbolic equations, namely, the linear advection equation and one-dimensional and two-dimensional Euler system of equations. In order to solve these equations, the Finite Volume Method was employed with an explicit formulation, Lax-Friedrichs flux, two numerical schemes, first-order and WENO, and Runge-Kutta method. We have presented an error and order analysis for both numerical schemes, in which the WENO scheme showed fifth-order accuracy in all problems, except with discontinuous solutions as expected. We also confirmed that the WENO scheme is less dissipative even with discontinuities and in coarse meshes.

Keywords: Verification, Hyperbolic conservation laws, WENO

1 INTRODUCTION

The verification is an important procedure in numerical methods that check accuracy and grants numerical reliability, lead by an error assessment that plays a fundamental role. Nonetheless, there are some works that do not present an error assessment and the numerical solution is obtained on a single mesh (Marchi and Hobmeir, 2007). Although one can assess the error on a single mesh, it is pertinent to evaluate the error behavior through some different meshes, for instance, to confirm that the solution is convergent. Furthermore, the verification can also evaluate how numerical procedures, e.g., numerical fluxes and schemes, behaves with different types of problems.

One of the most popular numerical schemes to solve hyperbolic conservation laws is the Weighted Essentially Nonoscillatory (WENO), that is a modification of the original Essentially Nonoscillatory (ENO) scheme (Liu et al., 1994). Since its first modification, this scheme was improved by several authors (see, for instance, Jiang and Shu (1996) and Henrick et al. (2005)) in order to correct some drawbacks and improve the resolution. In their work, Borges et al. (2008) proposed an improvement to WENO that required smaller computational effort and is less dissipative.

With regard to the above mentioned, the purpose of this work is to verify numerical codes and its solutions and to evaluate the WENO-Z (Borges et al., 2008) behavior in four different problems and different meshes. In order to do that, we employed an explicit formulation of the Finite Volume Method (FVM), Lax-Friedrichs flux and Runge-Kutta method for time discretization. Also, we solved the same problems with a first-order numerical scheme to better observe the WENO-Z features. The problems solved were linear advection equation and one-dimensional (1D) and two-dimensional (2D) Euler systems of equations. These equation belong to the class of hyperbolic conservation laws and can be written as

$$\mathbf{U}_t + \mathbf{F}(\mathbf{U})_x + \mathbf{G}(\mathbf{U})_y = \mathbf{0}, \quad (1)$$

where \mathbf{U} , $\mathbf{F}(\mathbf{U})$ and $\mathbf{G}(\mathbf{U})$ are the vectors of conserved variables and fluxes. Depending on the problem, they can be a scalar instead of a system and have only the $\mathbf{F}(\mathbf{U})$ component, if it is 1D.

2 NUMERICAL PROCEDURE

The numerical procedure is divided into two sections: the discretization will briefly shows the FVM setup for each problem and the verification will present an a priori error analysis to determine the asymptotic order of numerical schemes and an a posteriori technique to assess the error and effective order.

2.1 Discretization

We will first present the setup for a scalar one-dimensional problem and then some modifications for systems and two-dimensional problems. Consider a generic volume i , shown in Fig. 1. To apply the FVM one can use the method of lines approach and integrate the Eq. (1) over the volume to obtain Eq. (2) (Shu, 1998).

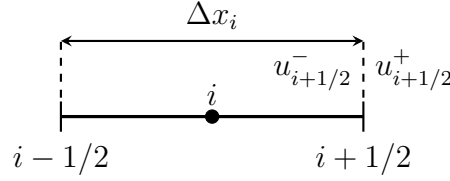


Figure 1: Generic volume i .

$$\frac{d\bar{u}(x_i, t)}{dt} = -\frac{1}{\Delta x_i} [f(u(x_{i+1/2}, t)) - f(u(x_{i-1/2}, t))], \quad (2)$$

where $\bar{u}(x_i, t)$ is the cell average, t is the time, Δx_i is the volume size in x direction and f is the flux.

According to Shu (1998), one needs to approximate Eq. (2) by a conservative scheme, such as

$$\frac{d\bar{u}_i(t)}{dt} = -\frac{1}{\Delta x_i} (\hat{f}_{i+1/2} - \hat{f}_{i-1/2}), \quad (3)$$

where $\bar{u}_i(t)$ is an approximation to the cell average and $\hat{f}_{i\pm 1/2}$ is the numerical approximation to the flux ($f(u(x_{i\pm 1/2}, t))$). One of the most simple albeit dissipative monotone flux is the Lax-Friedrichs flux

$$\hat{f}_{i+1/2}(u_{i+1/2}^-, u_{i+1/2}^+) = \frac{1}{2} [f(u_{i+1/2}^-) + f(u_{i+1/2}^+) - \alpha(u_{i+1/2}^+ - u_{i+1/2}^-)], \quad (4)$$

where $u_{i\pm 1/2}^\pm$ are reconstructed from the cell averages by the numerical schemes (WENO-Z or first-order) and $\alpha = \max_u |f'(u)|$ is the maximum absolute eigenvalue.

The first-order scheme is obtained from a Taylor series and is shown in Eq. (5) and (6).

$$u_{i+1/2}^- = u_i \quad (5)$$

$$u_{i+1/2}^+ = u_{i+1} \quad (6)$$

To apply the WENO-Z one has the following equation

$$u_{i+1/2}^- = \omega_0 \phi_0 + \omega_1 \phi_1 + \omega_2 \phi_2, \quad (7)$$

where ω are the nonlinear weights and ϕ are the polynomial approximations to $u_{i+1/2}^-$.

The nonlinear weights are (Borges et al., 2008)

$$\omega_k = \frac{\alpha_k}{\sum_{j=0}^2 \alpha_j}, \quad k = 0, \dots, 2 \quad (8)$$

and α_k are the unnormalized nonlinear weights, shown in sequence:

$$\alpha_k = d_k \left[1 + \left(\frac{\tau}{\beta_k + \epsilon} \right)^p \right], \quad k = 0, \dots, 2. \quad (9)$$

Where d_k are the ideal weights, τ is the global smoothness indicator, β_k are the local smoothness indicator, p is the power parameter and ϵ is the sensitivity parameter. In our case, $p = 2$ and $\epsilon = 10^{-40}$. The ideal weights and smoothness indicators are shown in the following equations:

$$d_0 = \frac{1}{10}, \quad d_1 = \frac{6}{10}, \quad d_2 = \frac{3}{10}, \quad (10)$$

$$\tau = |\beta_0 - \beta_2|, \quad (11)$$

$$\begin{aligned} \beta_0 &= \frac{13}{12}(u_{i-2} - 2u_{i-1} + u_i)^2 + \frac{1}{4}(u_{i-2} - 4u_{i-1} + 3u_i)^2, \\ \beta_1 &= \frac{13}{12}(u_{i-1} - 2u_i + u_{i+1})^2 + \frac{1}{4}(u_{i-1} - u_{i+1})^2, \\ \beta_2 &= \frac{13}{12}(u_i - 2u_{i+1} + u_{i+2})^2 + \frac{1}{4}(3u_i - 4u_{i+1} + u_{i+2})^2. \end{aligned} \quad (12)$$

To complete the scheme one needs the polynomial approximations, shown in Eq. (13). More details can be seen in Borges et al. (2008).

$$\begin{aligned} \phi_0 &= \frac{2u_{i-2} - 7u_{i-1} + 11u_i}{6}, \\ \phi_1 &= \frac{-u_{i-1} + 5u_i + 2u_{i+1}}{6}, \\ \phi_2 &= \frac{2u_i + 5u_{i+1} - u_{i+2}}{6}. \end{aligned} \quad (13)$$

One should note that Eq. (7) provides an approximation to $u_{i+1/2}^-$ with the five-point stencil $S = \{u_{i-2}, u_{i-1}, u_i, u_{i+1}, u_{i+2}\}$. To approximate $u_{i+1/2}^+$, the five-point stencil becomes $S = \{u_{i+3}, u_{i+2}, u_{i+1}, u_i, u_{i-1}\}$.

We will use periodic boundary conditions in all cases, since they are easy to impose. Consider a mesh with N_g real volumes. To impose the boundary condition at the left boundary ghost volumes, one needs to set the ghost volumes u_{-2}, u_{-1} and u_0 with u_{N_g-2}, u_{N_g-1} and u_{N_g} , respectively (LeVeque, 2002). The right ghost volumes must be imposed in a similar way, i.e., u_{N_g+1}, u_{N_g+2} and u_{N_g+3} with u_1, u_2 and u_3 , respectively.

The numerical flux, scheme and boundary conditions will provide a spatial discretization to Eq. (3) and to solve this equation one needs the time discretization. This can be done by an optimal third-order Strong Stability Preserving (SSP) Runge-Kutta method (Shu, 1998):

$$\begin{aligned} u^{(1)} &= u^n + \Delta t L(u^n) \\ u^{(2)} &= \frac{3u^n + u^{(1)} + \Delta t L(u^{(1)})}{4} \\ u^{n+1} &= \frac{u^n + 2u^{(2)} + 2\Delta t L(u^{(2)})}{3}, \end{aligned} \quad (14)$$

where the superscripts (1), (2), n and $n + 1$ are the first and second stages, the current time and the next time step, Δt is the time step size and $L(\cdot)$ is the spatial approximation to Eq. (3).

The procedure described above is suitable for scalar equations. In the case of nonlinear system of equations, such as Euler 1D and 2D, a characteristic variable decomposition is needed

(Shu, 1998):

$$\mathbf{W} = \mathbf{L}\mathbf{U}, \quad (15)$$

where \mathbf{W} and \mathbf{L} are the characteristic vector and the left eigenvectors.

Instead of approximating $u_{i+1/2}^{\pm}$, one needs to approximate each component of the characteristic variables and, after that, change back into conservative variables with

$$\mathbf{U} = \mathbf{R}\mathbf{W}, \quad (16)$$

where \mathbf{R} is the right eigenvectors. More details about the eigenvectors can be found in Toro (2009).

Finally, to solve the 2D Euler system of equations one can use the procedure for nonlinear system of equations in each direction and combine them in the following conservative scheme (Buchmüller and Helzel, 2014)

$$\frac{d\bar{u}_i(t)}{dt} = -\frac{1}{\Delta x_i}(\hat{f}_{i+1/2} - \hat{f}_{i-1/2}) - \frac{1}{\Delta y_i}(\hat{g}_{i+1/2} - \hat{g}_{i-1/2}), \quad (17)$$

where $\hat{g}_{i\pm 1/2}$ is the numerical flux in y direction.

As pointed by Buchmüller and Helzel (2014), this approach will only retain the WENO higher order for simple problems, which is our case. For more complex problems they suggest a modification, that will not be discussed here.

2.2 Verification

We consider only discretization errors in our analysis since we used high precision and no iterative schemes. To assess these errors we first need an a priori error analysis to obtain the error of the numerical schemes. This can be done via Taylor expansion, with the first order scheme and information from Fig. 1

$$u(x_{i+1/2}) = u(x_i) + u'(x_i)(x_{i+1/2} - x_i) + \frac{u''(x_i)}{2}(x_{i+1/2} - x_i)^2 + \dots \quad (18)$$

Clearly, the error for this approximation is $(x_{i+1/2} - x_i = \Delta x_i/2)$

$$E(u(x_{i+1/2})) = \frac{u'(x_i)}{2}\Delta x_i + \frac{u''(x_i)}{4}\Delta x_i^2 + \dots = O(\Delta x_i). \quad (19)$$

The asymptotic order (p_L) is the first power of Δx_i in the error equation. For the first-order scheme $p_L = 1$.

For the WENO-Z scheme, details of the Taylor series expansion can be found in Borges et al. (2008). Regarding that this scheme uses a polynomial reconstruction and a stencil combination to achieve higher orders, the fifth-order WENO-Z have $p_L = 5$.

In order to achieve convergence, one must confirm that apparent order (p_U) approaches the p_L monotonically in more than three meshes (Marchi and Silva, 2005). Since all problems

solved have analytical solutions, we will use the effective order (p_E) instead of p_U , which is given by

$$p_{E_g} = \frac{\log_{10}(L^1_{g-1}/L^1_g)}{\log_{10}(r)}, \quad g = 2, \dots, G, \quad (20)$$

where the subscript g refers to the mesh level, lower is coarse, $r = \Delta x_{i_{g-1}}/\Delta x_{i_g}$ is the refine ratio, G is the mesh quantity and L^1 is the norm of the error, computed from Eq. (21).

$$L^1_g = \sum_{i=1}^{N_g} \Delta x_{i_g} |E_i|, \quad g = 1, \dots, G. \quad (21)$$

Here, the error is the difference between exact and numerical solutions.

3 NUMERICAL EXPERIMENTS

The numerical codes used in this work were written in Fortran (standard 90 and higher) and compiled with Intel[®] Fortran 17 and all simulations were performed in one computer with Intel[®]Core[™] i7-4790 @ 3.6 GHz and 8 threads, 8 GB of RAM and Debian 9 operating system. Some of the simulations were parallelized using OpenMP. The main reason was to reduce the simulation time and for that purpose details will not be shown.

One should note that the Runge-Kutta has third-order accuracy in time and this should degenerate the solution accuracy order to three. To avoid this, the following time step must be used for the WENO-Z scheme:

$$\Delta t = \min(\Delta x_{i_g} \text{CFL}/\alpha, \Delta x_{i_g}^{5/3}), \quad (22)$$

where CFL is the Courant-Friedrichs-Lewy number.

3.1 Linear advection equation

In this section, we present the results for the linear scalar equation,

$$\begin{cases} u_t + u_x = 0 & x \in (-1, 1), \quad t > 0, \\ u(x, 0) = 0.25 + 0.5 \sin(\pi x) & x \in [-1, 1], \end{cases} \quad (23)$$

that has the exact solution (Tan and Shu, 2010)

$$u(x, t) = 0.25 + 0.5 \sin[\pi(x - t)]. \quad (24)$$

The domain was uniformly discretized,

$$\Delta x_g = \Delta x_{i_g} = \frac{x_r - x_l}{N_g}, \quad N_g = N2^{g-1}, \quad g = 1, \dots, G. \quad (25)$$

Here, $x_r = -1$ and $x_l = 1$ are the right and left boundary position, $G = 10$, $N = 20$ is the base mesh and N_g is the mesh volume quantity.

The L^1 norm of the discretization errors and its effective order at $t = 2$ are presented in Fig. 2 and 3, where we can see that the effective order is converging to the asymptotic as mesh is refined.

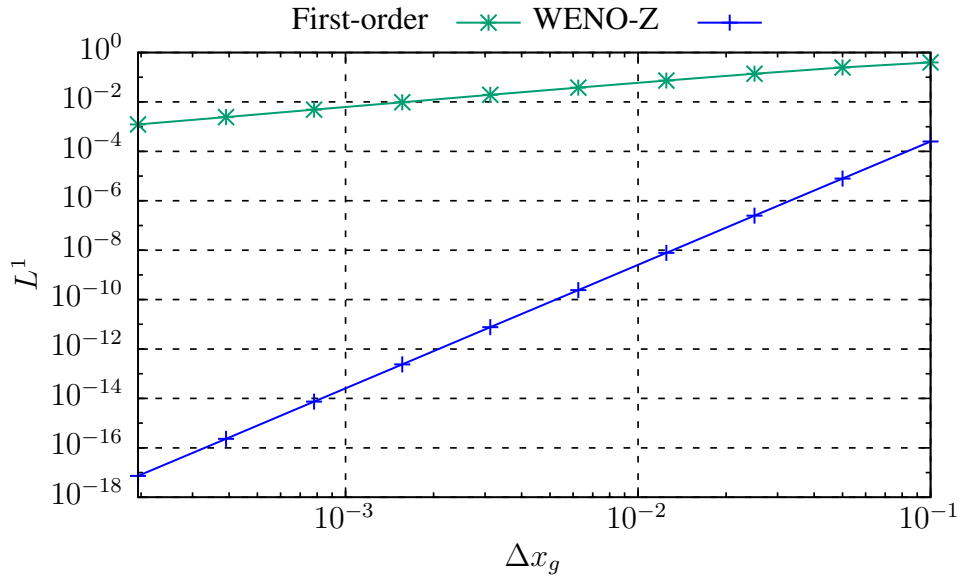


Figure 2: L^1 norm of the error for the linear advection equation at $t = 2$.

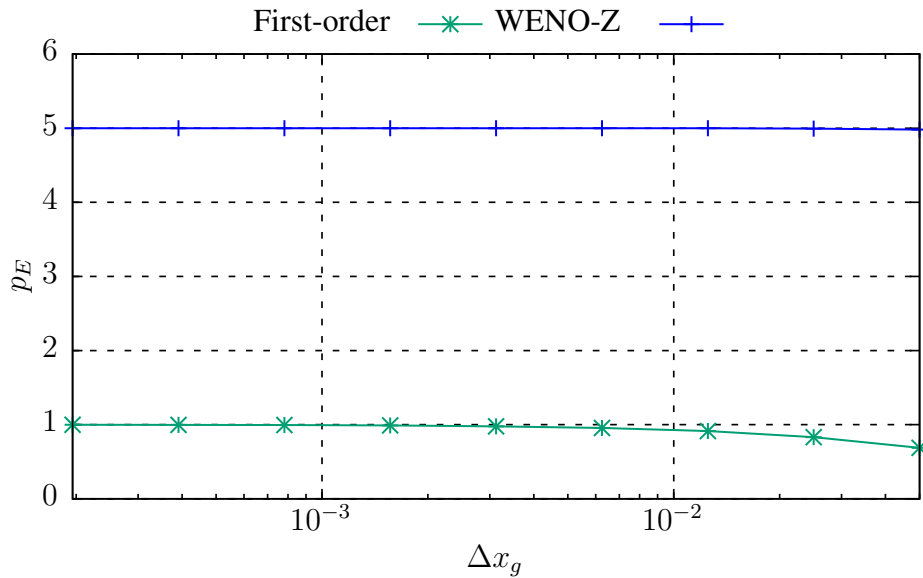


Figure 3: Effective orders of the L^1 norm for the linear advection equation at $t = 2$.

3.2 Euler 1D with smooth solutions

In this section, we present the results for the nonlinear 1D Euler system of equations with smooth solutions,

$$\begin{cases} \mathbf{U}_t + \mathbf{F}(\mathbf{U})_x = \mathbf{0} & x \in (-\pi, \pi), \quad t > 0, \\ \rho(x, 0) = 1 + 0.2 \sin(x), \quad u(x, 0) = 1, \quad p(x, 0) = 2 & x \in [-\pi, \pi], \end{cases} \quad (26)$$

with

$$\mathbf{U} = \begin{pmatrix} \rho \\ \rho u \\ E \end{pmatrix} \quad \text{and} \quad \mathbf{F}(\mathbf{U}) = \begin{pmatrix} \rho u \\ \rho u^2 + p \\ u(E + p) \end{pmatrix}, \quad (27)$$

where ρ is the density, u the velocity in the x direction, p is the pressure, E is the total energy per unit volume

$$E = \frac{\rho}{2}u^2 + \frac{p}{\gamma - 1} \quad (28)$$

and $\gamma = 1.4$ is the ratio of specific heats. More details on 1D Euler system of equations can be found in Toro (2009).

The exact solution for this problem is (Tan and Shu, 2010)

$$\rho(x, t) = 1 + 0.2 \sin(x - t), \quad u(x, t) = 1, \quad p(x, t) = 2. \quad (29)$$

The domain was uniformly discretized with Eq. (25), $N = 20$, $G = 10$, $x_l = -\pi$ and $x_r = \pi$.

The L^1 norm of discretization errors of the density and its effective order at $t = 2$ are presented in Fig. 4 and 5, where we can see that the effective order is converging to the asymptotic as mesh is refined.

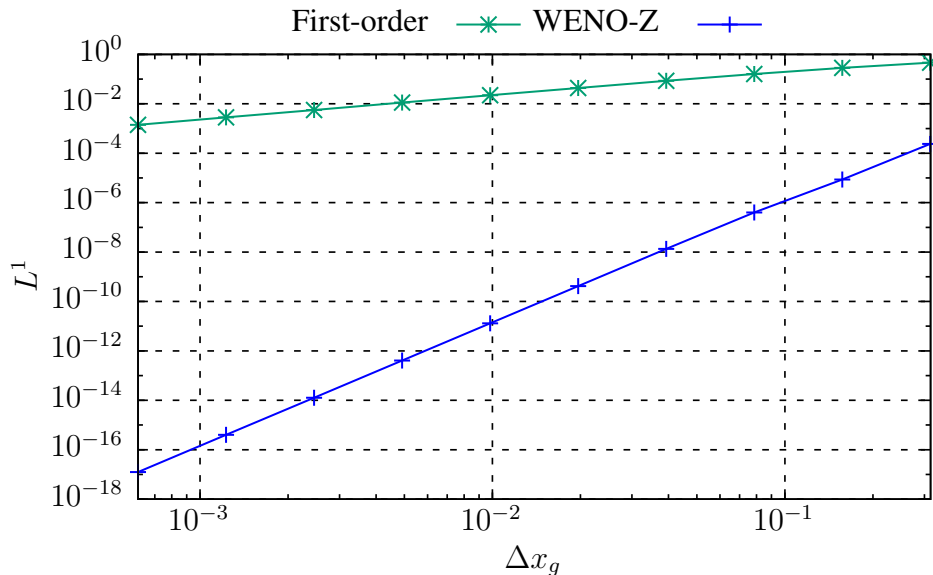


Figure 4: L^1 norm of the error for the 1D Euler system of equations with smooth solution and $t = 2$.

3.3 Euler 1D with discontinuous solutions

In this section, we present the results for the nonlinear 1D Euler system of equations with discontinuous solutions that have the following initial conditions

$$\begin{cases} \rho(x, 0) = -0.8(x + 0.5) + 0.7, & \text{if } -0.5 \leq x \leq 0 \\ u(x, 0) = 1, \quad p(x, 0) = 2 \\ \rho(x, 0) = 0.3, \quad u(x, 0) = 1, \quad p(x, 0) = 2 & \text{otherwise} \end{cases} \quad (30)$$

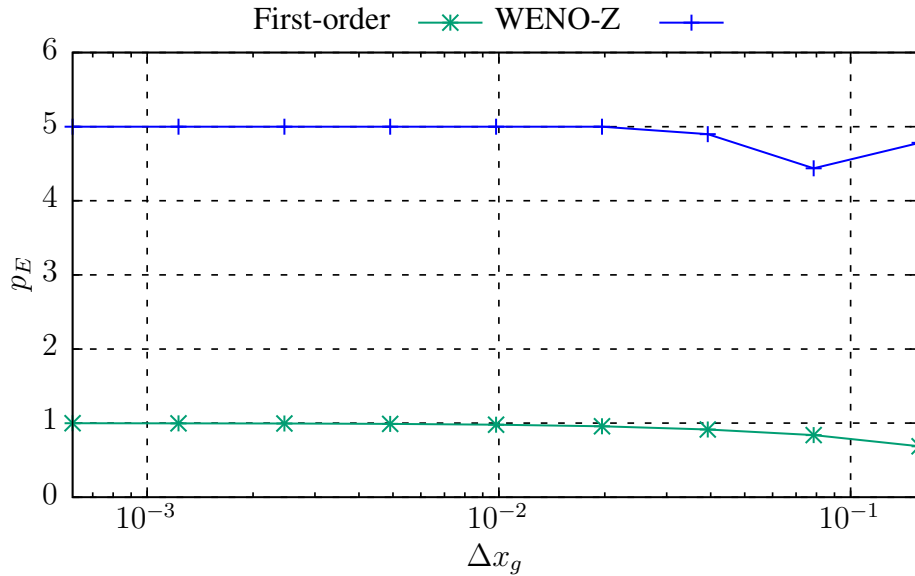


Figure 5: Effective orders of the L^1 norm for the 1D Euler system of equations with smooth solution and $t = 2$.

For $t < 1$, the exact solution for this problem is

$$\begin{cases} \rho(x, t) = -0.8(x + 0.5 - t) + 0.7, & \text{if } -0.5 + t \leq x \leq 0 + t \\ u(x, t) = 1, \quad p(x, t) = 2 & \\ \rho(x, t) = 0.3 \quad u(x, t) = 1 \quad p(x, t) = 2 & \text{otherwise} \end{cases} \quad (31)$$

The domain was uniformly discretized with Eq. (25), $N = 20$, $G = 10$, $x_l = -1$ and $x_r = 1$.

Exact and numerical solutions of the density for the first order and WENO-Z in the coarse mesh are presented in Fig. 6. One can note that the WENO-Z produces solutions with much less dissipation than the first order scheme and is close to the exact solution even with discontinuities and in coarse meshes.

The L^1 norm of the discretization errors of the density and its effective order at $t = 0.5$ are presented in Fig. 7 and 8, where the orders are converging to a value below the asymptotic order. This is an expected behavior since near the shock is a high dissipation region.

Figure 9 shows the error behavior near the discontinuity. Note the error increase as the solution approaches the discontinuity.

3.4 Euler 2D

In this section, we present the results for the nonlinear 2D Euler system of equations,

$$\begin{cases} \mathbf{U}_t + \mathbf{F}(\mathbf{U})_x + \mathbf{G}(\mathbf{U})_y = \mathbf{0}, & (x, y) \in (0, 1) \times (0, 1), \quad t > 0, \\ \rho(x, y, 0) = 1 + 0.5 \sin(2\pi x) \cos(2\pi y), & u(x, y, 0) = v(x, y, 0) = p(x, y, 0) = 1 \end{cases} \quad (32)$$

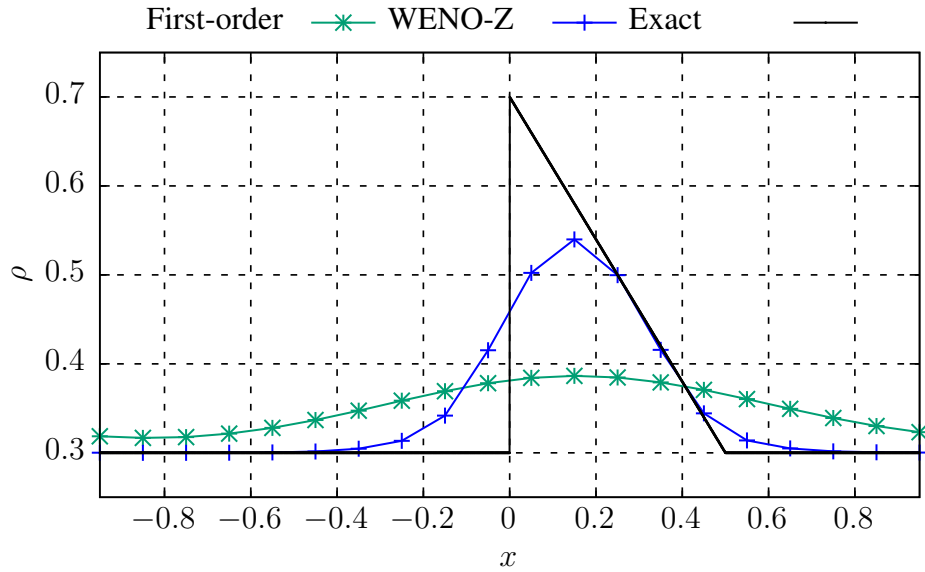


Figure 6: Exact and numerical solutions for the 1D Euler system of equations in the coarse mesh with discontinuous solution and $t = 0.5$.

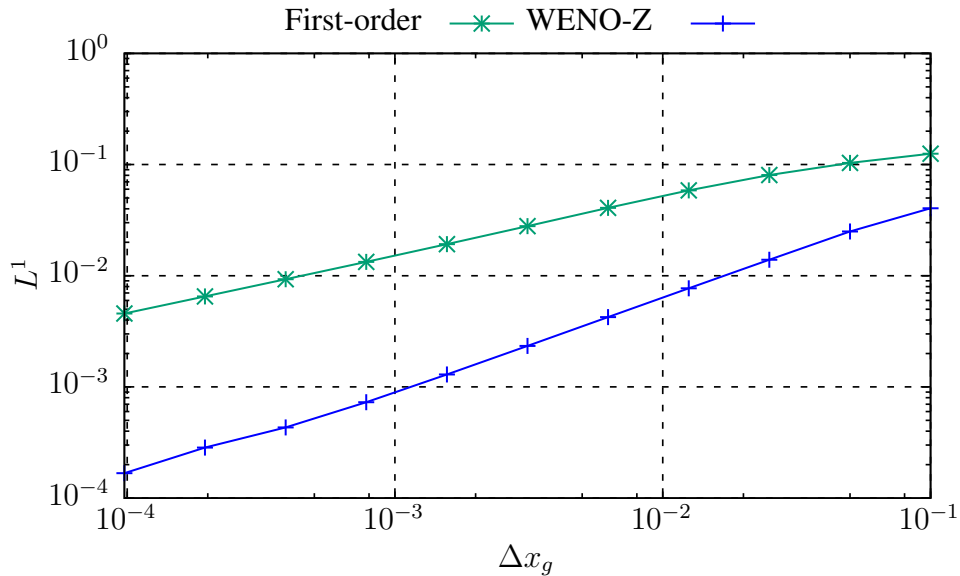


Figure 7: L^1 norm of the error for the 1D Euler system of equations with discontinuous solution and $t = 0.5$.

with

$$\mathbf{U} = \begin{pmatrix} \rho \\ \rho u \\ \rho v \\ E \end{pmatrix}, \quad \mathbf{F}(\mathbf{U}) = \begin{pmatrix} \rho u \\ \rho u^2 + p \\ \rho uv \\ u(E + p) \end{pmatrix}, \quad \mathbf{G}(\mathbf{U}) = \begin{pmatrix} \rho v \\ \rho uv \\ \rho v^2 + p \\ v(E + p) \end{pmatrix}, \quad (33)$$

where v is the velocity in the y direction and

$$E = \frac{\rho}{2}(u^2 + v^2) + \frac{p}{\gamma - 1}. \quad (34)$$

More details on 2D Euler system of equations can be found in Toro (2009).

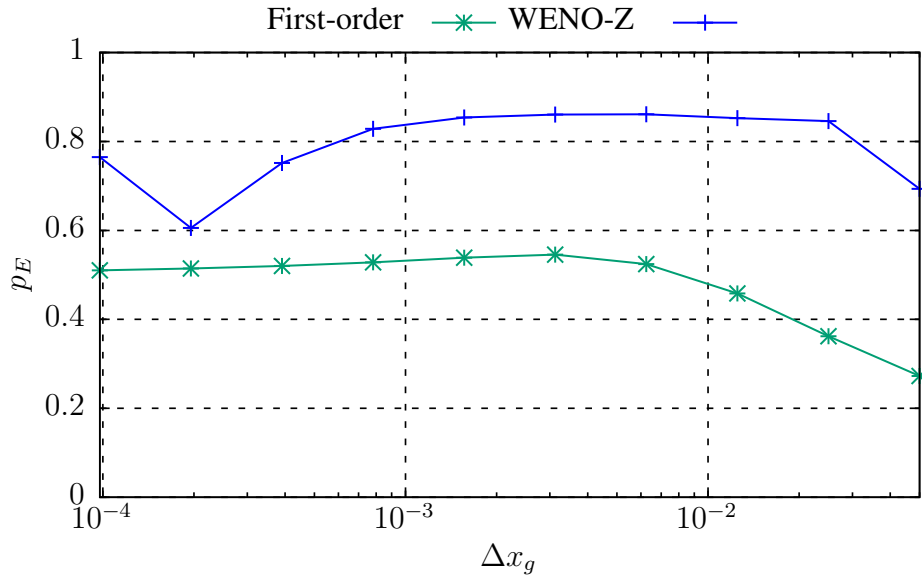


Figure 8: Effective orders of the L^1 norm for the 1D Euler system of equations with discontinuous solution and $t = 0.5$.

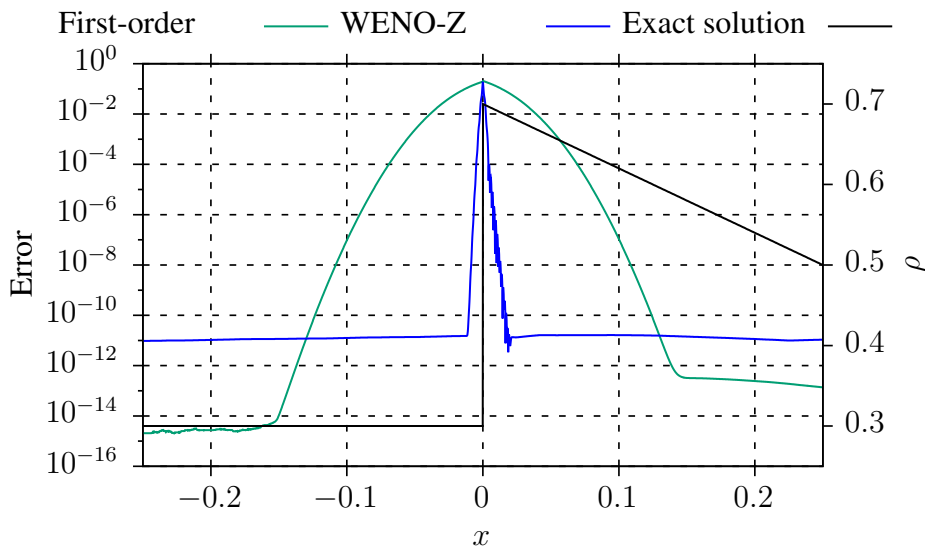


Figure 9: Error behavior near the discontinuity at $t = 0.5$.

The exact solution for this problem is

$$\rho(x, y, t) = 1 + 0.5 \sin[2\pi(x - t)] \cos[2\pi(y - t)], \quad u(x, t) = u(v, t) = p(x, t) = 1. \quad (35)$$

The domain was uniformly discretized in each direction with Eq. (25), $N = 20$, $G = 6$, $x_l = 0$, $x_r = 1$, $y_b = 0$ and $y_t = 1$, where y_b and y_t are the bottom and top boundaries in y direction.

For the 2D Euler system of equations we used the following L^1 norm

$$L_g^1 = \Delta x_g \Delta y_g \sum_{i=1}^{N_g N_g} |E_i|, \quad g = 1, \dots, G. \quad (36)$$

The L^1 norm of the discretization errors of the density and its effective order at $t = 2$ are presented in Fig. 10 and 11, where we can see that the effective order is converging to the asymptotic as mesh is refined.

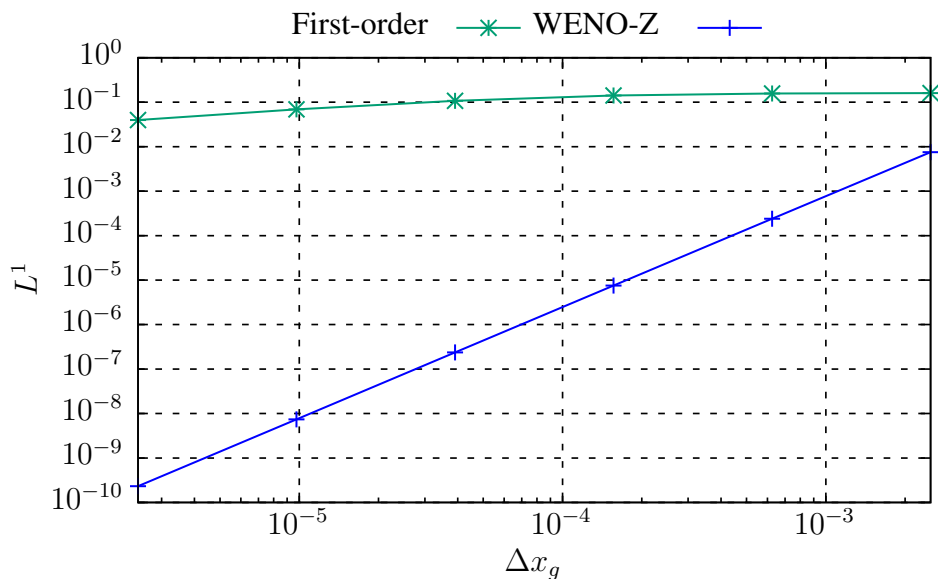


Figure 10: L^1 norm of the error for the 2D Euler system of equations at $t = 2$.

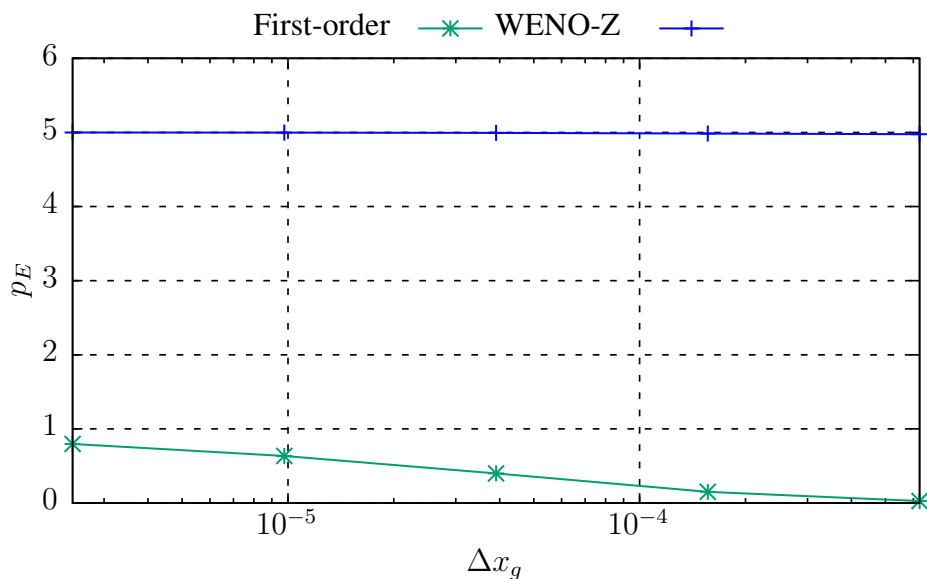


Figure 11: Effective orders of the L^1 norm for the 2D Euler system of equations at $t = 2$.

4 CONCLUDING REMARKS

We briefly presented the discretization for an explicit FVM formulation with Lax-Friedrichs flux, first-order and WENO-Z numerical schemes and an optimal third-order SSP Runge-Kutta method suitable for hyperbolic conservation laws, such as the Euler equations. The solution of each problem is reliable as depicted by the verification procedure.

We showed that the WENO-Z solution is close to the exact even with discontinuities and in coarse meshes. This is an important behavior for shock-capturing schemes.

In most of the problems, the WENO-Z presented fifth-order accuracy. Although expected, in the case of 1D Euler system of equations with discontinuous solutions the order degenerates. This happens because the WENO-Z scheme selects the smoothest combination of the substencils, which may not achieve higher order, and because of the high dissipation effect near the discontinuity.

ACKNOWLEDGEMENTS

We would like to thank the CAPES (Coordination for the Improvement of Higher Education Personnel), CNPq (National Counsel of Technological and Scientific Development), PG-Mec (Postgraduate Program in Mechanical Engineering) and DEMEC (Department of Mechanical Engineering) for their financial support. The first author is supported by a CAPES scholarship and the third by a CNPq scholarship.

REFERENCES

- Borges, R., Carmona, M., Costa, B., & Don, W. S., 2008. An improved weighted essentially nonoscillatory scheme for hyperbolic conservation laws. *Journal of Computational Physics*, vol. 227, n. 6, p. 3191-3211.
- Buchmüller, P., & Helzel, C., 2014. Improved accuracy of high-order WENO Finite Volume Methods on cartesian grids. *Journal of Scientific Computing*, vol. 61, n. 2, pp. 343-368.
- Henrick, T. D., Aslam, J. M., & Powers, J. M., 2005. Mapped weighted essentially non-oscillatory schemes: achieving optimal order near critical points. *Journal of Computational Physics*, vol. 207, n. 2, p. 542-567.
- Jiang, G. S., & Shu, C. W., 1996. Efficient implementation of weighted ENO schemes. *Journal of Computational Physics*, vol. 126, n. 1, p. 202-228.
- LeVeque, R. J., 2002. Finite Volume Methods for hyperbolic problems. *Cambridge University Press*.
- Liu, X. D., Osher, S., & Chan, T., 1994. Weighted essentially non-oscillatory schemes. *Journal of Computational Physics*, vol. 115, n. 1, p. 200-212.
- Marchi, C. H., & Hobmeir, M. A., 2007. Numerical solution of staggered circular tubes in two-dimensional laminar forced convection. *Journal of the Brazilian Society of Mechanical Sciences and Engineering*, vol. 29, n. 1, p. 42-48.
- Marchi, C., H., & Silva, A. F. C., 2005. Multi-dimensional discretization error estimation for convergent apparent order. *Journal of the Brazilian Society of Mechanical Sciences and Engineering*, vol. 27, n. 4, p. 432-439.
- Toro, E. F., 2009. Riemann solvers and numerical methods for fluid dynamics: a practical introduction. *Springer-Verlag Berlin Heidelberg*.
- Tan, S., & Shu, C. W., 2010. Inverse Lax-Wendroff procedure for numerical boundary conditions of conservation laws. *Journal of Computational Physics*, vol. 229, n. 21, p. 8144-8166.
- Shu, C. W., 1998. Essentially non-oscillatory and weighted essentially non-oscillatory schemes for hyperbolic conservation laws. *Advanced Numerical Approximation of Nonlinear Hyperbolic Equations*, vol. 1697, pp. 325-432.